Quasiparticle-random-phase approximation treatment of the transverse wobbling mode reconsidered

S. Frauendorf* and F. Dönau†
Department of Physics, University of Notre Dame, South Bend, Indiana 46556, USA
(Received 5 October 2015; published 10 December 2015)

The quasiparticle-random-phase approximation is used to study the properties of the wobbling bands in ^{163}Lu. Assuming that the wobbling mode represents pure isoscalar orientation oscillations results in too low wobbling frequencies and transition probabilities between the one- and zero-phonon wobbling bands that are strongly collective but yet too weak for $B(E2)_{\rm out}$ and too strong for $B(M1)_{\rm out}$. The inclusion of an LL interaction, which couples the wobbling mode to the scissors mode, generates the right upshift of the wobbling frequencies and the right suppression of the $B(M1)_{\rm out}$ values toward the experimental values, but does not change the $B(E2)_{\rm out}$ values. In analogy to the quenching of low-energy $E1$ transition by coupling to the isovector giant dipole resonance, a general reduction of the $M1$ transitions between quasiparticle configurations caused by coupling to the scissors mode is suggested. The small $\mathrm{B}(E2)_{\rm out}$ values are related to small triaxiality of the density distribution, which is found by all mean field calculations for the triaxial strongly deformed nuclei in the mass 160 region.

DOI: 10.1103/PhysRevC.92.064306 PACS number(s): 21.10.Re, 23.20.Lv, 27.70.+q

I. INTRODUCTION

Rotating nuclei that have a triaxially deformed shape are expected to exhibit a characteristic excitation mode called "wobbling" by Bohr and Mottelson [1], which is an orientation vibration of the triaxial body about the rotational axis. It is the nuclear analog to the motion of the classical top with three different moments of inertia, which is well known from the rotational spectra of molecules. Experimental evidence for the wobbling mode was established by the discovery [2–4] of rotational bands in the ^{71}Lu isotopes when they attain a triaxial strongly deformed (TSD) shape at high spin. The simple dynamics of a rotor with three different moments of inertia results in an increase of the wobbling frequency with angular momentum, which is seen in molecules. However, for the Lu isotopes a decrease is observed, which makes the identification of the wobbling possible, because it prevents the mode being fragmented among competing quasiparticle excitations. In the framework of the quasiparticle+triaxial-rotor (QTR) model, Frauendorf and Dönau [5] demonstrated that the decrease results from the presence of the odd $\mathrm{i}_{13/2}$ quasiproton, which aligns its angular momentum along the short body axis, *transverse* to the medium axis with the largest moment of inertia. To notify the modification of the dynamics by the odd quasiparticle, they introduced the name "transverse wobbling." They predicted the appearance of transverse wobbling for the mass 130 region, where the $\mathrm{h}_{11/2}$ quasiparticle couples transverse to the triaxial rotor. The prediction was recently confirmed for ^{135}Pr [6]. The QTR calculations well account for the wobbling energies and the $B(E2)_{\rm out}$ values of the $\Delta I = 1$ electric quadrupole transitions, which connect the one-phonon wobbling band with the zero-phonon band. However, the $B(M1)_{\rm con}$ values of the connecting magnetic dipole transitions are overestimated by about a factor of 3–10 (see Refs. [6] and [5]). The discrepancy turns out to be robust, and it can be traced back to the transverse geometry: For a quasiproton that is rigidly coupled to the triaxial charge density distribution (HFA approximation of Ref. [5]) the amplitude of the wobbling vibrations of the charge density, which generate the $B(E2)_{\rm out}$ values of the interband transitions, determines the amplitude of the vibrations of the magnetic moment of the odd quasiproton, which generate the $B(M1)$ values of the interband transitions. Realistically, the odd quasiproton is not rigidly coupled to the rotor, which reduces the amplitude of the oscillations of the magnetic moment and thus the $B(M1)_{\rm out}$ values. However, the reduction is too weak to bring down the $B(M1)_{\rm out}$ to the experimental values (see Fig. 19 of Ref. [5]). The present paper addresses this problem of the too strong magnetic dipole transitions from a microscopic perspective.

Following the discovery of the first wobbling structure in ^{163}Lu [2], Ødegård *et al.*, Hamamoto, and Hamamoto and Hagemann [2,7,8] used the QTR model to describe the wobbling mode. These calculations made the *ad hoc* assumption that the short axis has the largest moment of inertia, by exchanging the hydrodynamic moments of inertia of the short and medium axes. The large ratios $B(E2)_{\rm out}/B(E2)_{\rm in}$ of interband to intraband $E2$ transitions could be well reproduced. The $B(M1)_{\rm out}$ were only overestimated by a factor of 2–3. However, the calculated wobbling frequencies of the QTR model with the "inverted moments of inertia" assumption distinctly disagree with experiment. Instead of the experimentally observed decrease, the wobbling frequency increases with the spin I, which is expected because the inverted moment of inertia arrangement corresponds to the longitudinal wobbling geometry in the terminology of Ref. [5]. Reference [9] suggested remedying the problem by assuming a decrease of the scale of the rotational energy, which may reflect the increase of the moments of inertia from a reduction of the pair correlations. In our view, the "inverted moments of inertia" assumption is unrealistic because any microscopic calculation of the three moments of inertia in the frame of

*sfrauend@nd.edu
†Deceased.

the cranking model give the maximal moment of inertia for the medium axis. This result is in accordance with the hydrodynamic ratios between the moments of inertia. It can be qualitatively understood by the fact that the moment of inertia of a certain axis increases with the deviation from cylindric symmetry, which is maximal for the medium axis. Hence, the problem with the too strong magnetic transition remains.

The observation of the wobbling mode stimulated theoretical efforts to understand how the nuclear shell structure and the residual interaction generate such a type of collective excitations. Matsuyanagi, Matsuzaki, Ohtsubo, Shimizu, and Shoji demonstrated that the quasiparticle-random-phase approximation (QRPA) is an adequate microscopic approach [10–14]. QRPA describes wobbling bands in terms of correlated two-quasiparticle excitations in a rotating triaxial potential. Relevant results of these studies can be summarized as follows.

(1) The QRPA calculations agree with the transverse wobbling geometry as discussed in Ref. [5]. The authors refers to it as "positive γ shape," which uses the common terminology of principle axis cranking that assigns the sector $0 \leqslant \gamma \leqslant 60^\circ$ to rotation about the short axis. The angular momentum of the odd $i_{13/2}$ quasiparticle aligns with this axis. The decrease of the wobbling frequency is interpreted as the approach of the instability of the cranking solution to a tilt of the rotational axis into the short-medium plane, which is signaled by the frequency of the lowest QRPA solution becoming zero [12].

(2) The collective enhancement of the connecting $E2$ transitions is born out. QRPA calculations underestimate the ratios $B(E2)_{\rm out}/B(E2)_{\rm in}$ by about a factor of two [10–13].

(3) The $B(M1)_{\rm out}$ values of the interband transitions are overestimated by a factor of 10 as for the QTR results for transverse wobbling.

The QRPA calculations [10–13] used a residual interaction of the isoscalar quadrupole-quadrupole (QQ) type. Because such interaction generates the same coupling between the odd quasiparticle and the triaxial rotor core as in the QTR calculations, it comes as no surprise that both approaches overestimate $B(M1)_{\rm out}$ values by the same factor. The reason to revisit the QRPA in this paper is to investigate how modifying the residual interaction influences the resulting excitation energies and electromagnetic transition rates. In particular we are interested whether the suppression of the interband $M1$ transitions can be obtained for transverse wobbling. We study the $i_{13/2}$ TSD bands in ^{163}Lu which offer the most complete set of data.

Our QRPA calculations are carried out in the uniformly rotating (UR) frame of reference. They are equivalent with the QRPA in the system of body fixed axes (PA), which was used in Refs. [10–12]. The QRPA equations in the PA system become very similar to the equations for the wobbling mode of the triaxial rotor (TR) model when the phenomenological moment of inertia are replaced by the appropriate microscopic expressions. This lends an intuitive interpretation of the QRPA results and makes contact with the triaxial rotor phenomenology. In particular, the geometry of transverse wobbling appears as a decrease with spin of the moment of inertia of the short axis [cf. Eq. (15) of Ref. [5]]. The transformation between the two versions of QRPA is discussed in Ref. [13], which carries out the QRPA in the uniformly rotating frame and interprets the results in the body-fixed frame. An alternative way of connecting the QRPA with the triaxial rotor was taken by Ref. [15], which uses the equivalence of QRPA and small amplitude TDHF theory to separate the motion of the quadrupole tensor with respect to the UR frame into oscillations of its orientation, the wobbling mode, and oscillations of the shape. (The more general case of chiral vibrations is considered, which includes wobbling as a special case.)

The paper is organized as follows. In Sec. II A a self-consistent treatment of the QRPA is performed by deriving the shape parameters (ε,γ) from the QQ interaction. In Sec. II B the shape parameters (ε,γ) are adopted from a Nilsson-Strutinsky minimization and the strength of residual QQ interaction is determined by restoring the rotational invariance of the Hamiltonian. Section III studies the consequences of additional interactions. Coupling to the low-energy orbital $M1$ resonance ("scissors mode") is suggested as a mechanism that suppresses the strength of the $M1$ interband transitions. Section IV summarizes the results and puts them into perspective.

II. QUASIPARTICLE-RANDOM-PHASE APPROXIMATION (QRPA) FOR ISOSCALAR QQ INTERACTION

A. Self-consistent QRPA (sc QRPA) with standard QQ interaction

The theoretical framework of our QRPA calculations is similar to the one used in our recent study of chiral vibrations [15]. The Hamiltonian $\hat{H}'$ is defined with respect to a reference system uniformly rotating about the 1-axis,

$$\hat{H}' = \hat{H} - \omega \hat{J}_1, \tag{1}$$

where ω is the cranking frequency and $\hat{J}_1$ denotes the 1-component of the angular momentum operator. The cranking term $-\omega \hat{J}_1$ ensures that the states have an average angular momentum $\langle J_1 \rangle = I$. The corresponding laboratory Hamiltonian $\hat{H}$ in Eq. (1) is

$$\hat{H} = \sum_{\tau=\pi,\nu} \left[\hat{h}^\circ_\tau - \Delta_\tau(\hat{P}^\dagger_\tau + \hat{P}_\tau) - \lambda_\tau \hat{N}_\tau\right] - \frac{\kappa_0}{2} \sum_{m=-2,2} (-1)^m \hat{Q}_m \hat{Q}_{-m}. \tag{2}$$

The operator $\hat{h}^\circ_\tau$ is the spherical part of the Nilsson Hamiltonian where the isospin index $\tau = \pi,\nu$ distinguishes the neutron and proton contributions, respectively. The term $\Delta_\tau(\hat{P}^\dagger_\tau + \hat{P}_\tau)$ accounts for the pair field where $\hat{P}^\dagger_\tau$ and $\hat{P}_\tau$ are the familiar monopole pair operators. Aiming at the high-spin $\pi i_{13/2}$ band in ^{163}Lu, the gap parameters Δ_τ are assumed to be reduced: Below the cranking frequency $\omega = 0.45$ MeV we take $\Delta_\pi = 0.45$ MeV for the proton gap and $\Delta_\nu = 0.35$ MeV for the neutron gap, and we use $\Delta_{\tau=\pi,\nu} = 0$ above. As usual, the terms $\lambda_\tau \hat{N}_\tau$, containing the particle number operators $\hat{N}_\tau$, are introduced to attain the average particle numbers $\langle \hat{N}_\pi \rangle = Z$ and $\langle \hat{N}_\nu \rangle = N$, respectively, by an appropriate choice of the Fermi energy λ_τ. The following term in Eq. (2) is the isoscalar quadrupole-quadrupole (ISQQ) interaction. It is constructed from the mass quadrupole operators $\hat{Q}_m = \hat{Q}_m(\pi) + \hat{Q}_m(\nu)$,

where $\hat{Q}_m(\tau) \equiv \sqrt{4\pi/5}\ (r/b_\circ)^2 Y_{2m}(\tau)$, and $b_\circ = 1.01A^{1/3}$ is the oscillator length. The model space is restricted to the oscillator shells $N = 4,5,6$, and the matrix elements between different N are discarded. It should be underlined that the latter assumptions are an essential part defining our model. They imply the use of polarization charges, for which we adopted the values $e_p = (1 + \mathrm{Z/A})e$ and $e_n = \mathrm{Z/A}\, e$ for the proton and neutron parts of the electric quadrupole operator.

In this section we follow the standard scheme requiring self-consistency between the ISQQ interaction and the deformed nuclear shape, which is defined by the parameters (ε,γ). More precisely, it is the deformed mean field potential v of the ISQQ interaction which, for a predefined interaction strength κ_0, has to obey the condition,

$$v = v(\varepsilon,\gamma) = -\kappa_0[\langle\hat{Q}_0\rangle\hat{Q}_0 + \langle\hat{Q}_2\rangle(\hat{Q}_2 + \hat{Q}_{-2})], \qquad (3)$$

where $|\rangle = |\,\varepsilon,\gamma\rangle$ is the quasiparticle reference state of the $\pi i_{13/2}$ TSD band as specified below. Denoting the c numbers $\langle\hat{Q}_{0,2}\rangle$ as $q_{0,2}(\varepsilon,\gamma)$ the self-consistency conditions demand searching for deformation parameters which at a given cranking frequency ω satisfy the relations,

$$\begin{aligned}\kappa_0\langle\hat{Q}_0\rangle &\equiv \kappa_0 q_0(\varepsilon,\gamma) = \quad 2/3\,\hbar\omega_0\,\varepsilon\cos\gamma,\\ \kappa_0\langle\hat{Q}_2\rangle &\equiv \kappa_0 q_2(\varepsilon,\gamma) = -2/3\,\hbar\omega_0\,\varepsilon\sin\gamma/\sqrt{2}.\end{aligned} \qquad (4)$$

The mean field calculations are done by using the tilted axis cranking (TAC) code described in Ref. [16]. It should be noted that the above conditions lead to a stable equilibrium shape only if one renders the volume conservation by taking the scale factor $\hbar\omega_0 = 41A^{-1/3}$ MeV as constant. Combining the spherical mean field part from the Hamiltonian $\hat{H}'$, Eq. (1), with the self-consistency conditions (4), one obtains the mean field Hamiltonian of the standard principle axis cranking (PAC) model $\hat{h}' = \hat{h} - \omega\hat{J}_1$ [16], where $\hat{h}$ is given by

$$\begin{aligned}\hat{h} = \hat{h}^\circ - \Delta_\tau(\hat{P}^\dagger + \hat{P}) - \lambda\hat{N}\\ - \hbar\omega_0\frac{2}{3}\varepsilon\left(\cos\gamma\,\hat{Q}_0 - \frac{\sin\gamma}{\sqrt{2}}(\hat{Q}_2 + \hat{Q}_{-2})\right).\end{aligned} \qquad (5)$$

The diagonalization of the PAC Hamiltonian $\hat{h}$ is done in an oscillator basis with the quantum numbers $\{n,l,j,m\}$ including the orbits of the three main shells $N = 4$–6. The search for the equilibrium needs to be performed with diabatic tracing (c.f. [16]) of the selected $(\pi i_{13/2}, \nu\ \mathrm{g})$ configuration of the TSD band. The strength of the sc ISQQ interaction $\kappa_0 = 0.019\,60$ MeV is ω independent and chosen such that at $\omega = 0.15$ MeV/$\hbar$ the deformation parameter comes close to the suggested value $\varepsilon = 0.4$ of the experimental TSD band [17]. The self-consistent deformation parameters for the frequency interval $\omega = 0.15$–0.50 MeV/$\hbar$ are presented in Table I. It is seen that for the ISQQ interaction the self-consistent triaxiality parameter $\gamma \approx 9^\circ$–12° is lower than $+20^\circ$ found in Ref. [17] by means of Nilsson-Strutinsky minimization. The relative change of the deformation (ε,γ) to higher rotational frequencies is small. Nevertheless precise self-consistency is required in the subsequent QRPA calculation to obtain reliable values for the excitation energies and $E2/M1$ properties of the wobbling band. As already noted in the previous QRPA papers [10–14], the absolute minimum of $\langle\hat{H}'\rangle$ corresponds to rotation about the short axis of the triaxial potential, along which the angular momentum of the $i_{13/2}$ proton is aligned (the sector of positive γ values in standard PAC terminology). Above the frequency $\omega = 0.5$ MeV/$\hbar$ the PAC solution becomes unstable, because the moment of inertia of the medium axis is larger than the one of the short axis. The stable solution corresponds to rotation about a *tilted* axis in the short-medium plane, which represents a $\Delta I = 1$ band. The QRPA frequency goes to zero when approaching the instability from below. Thus, the QRPA solution studied in this paper is of the "transverse wobbling" type according to the classification scheme introduced by us in Ref. [5], where the corresponding physics is discussed in the semiclassical framework of the HFA approximation.

TABLE I. Equilibrium values of the deformation parameters (ε,γ) in the frequency region $\omega = 0.15$–0.50 MeV/$\hbar$. The strength parameter of the ISQQ interaction is $\kappa_0 = 0.019\,60$ MeV.

ω(MeV/$\hbar$)	ε	γ(deg)
0.15	0.398 839	9.248
0.20	0.397 926	9.362
0.25	0.396 632	9.486
0.30	0.394 788	9.631
0.35	0.392 064	9.798
0.40	0.387 658	9.977
0.45	0.381 236	11.575
0.50	0.377 065	11.619

In Fig. 1 we show the total Routhian surface for $\omega = 0.45$ MeV/$\hbar$ as obtained by diabatic tracing the TSD configuration with the TAC code. The ISQQ interaction gives a relatively shallow minimum on the deformation surface. In Fig. 2 the experimental and calculated moments of inertia $\mathcal{J}^{(1)}$ are compared. The experimental frequencies of the TSD bands are derived by using the standard definition $\omega(\bar{I}) = (E(I) - E(I-2))/2$, where transition spin $\bar{I} = I - 1/2$, and the experimental moment of inertia $\mathcal{J}^{(1)}(\bar{I}) = \bar{I}//\omega(\bar{I})$. The calculation somewhat overestimates the experimental values.

Figure 3 presents the experimental $B(E2)_{\mathrm{in}}$ values of the $I \to I-2$ transitions within the TSD g band [17] and the ones calculated with the self-consistent TAC model. Starting

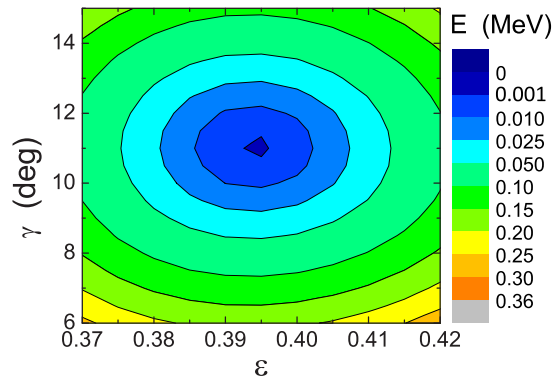

FIG. 1. (Color online) Total Routhian surface for the TSD configuration in ^{163}Lu at $\omega = 0.45$ MeV/$\hbar$.

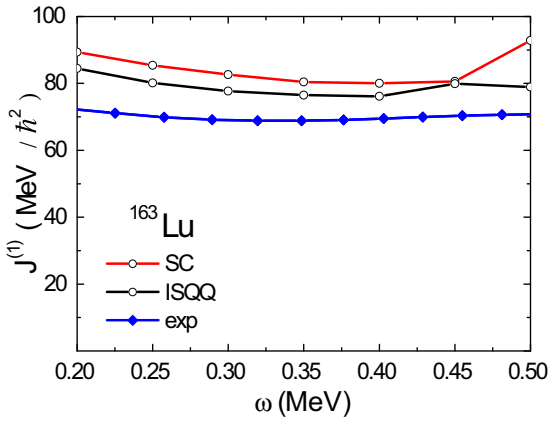

FIG. 2. (Color online) Experimental and calculated kinematic moments of inertia of the TSD band in ^{163}Lu. The calculated moment of inertia is $\mathcal{J}^{(1)} = \langle J_1 \rangle / \omega$.

from results of the self-consistent TAC calculation the QRPA is performed following the general formalism as outlined in the textbooks (e.g., [18]). We mention only the important steps of the QRPA and refer for more details to our recent paper [15]. First, the Hamiltonian (1) is rewritten in quasiparticle (qp) representation,

$$\hat{H}' = \hat{h}' + \hat{V}_{4qp}, \tag{6}$$

where $\hat{h}'$ is the diagonalized TAC Hamiltonian,

$$\hat{h}' = E_\circ + \sum_i e_i \hat{\alpha}_i^\dagger \hat{\alpha}_i. \tag{7}$$

The set $\{\hat{\alpha}_i^\dagger, \hat{\alpha}_i\}$ denotes the qp operators, e_i are the qp energies, and $\hat{V}_{4qp}$ contains the residual 4qp interaction terms which give rise to the vibrational excitations. Then, the quasiboson approximation $\hat{\alpha}_i^\dagger \hat{\alpha}_j^\dagger \Rightarrow \hat{b}_{ij}^\dagger$ is applied such that the Hamiltonian, Eq. (6), is expressed in terms of bosons, $\hat{H}' \Rightarrow \hat{H}'_{\rm RPA}$, keeping only boson terms up to second order [18]. This Hamiltonian is diagonalized by using the QRPA equation,

$$[\hat{H}'_{\rm QRPA},\ \hat{O}_\lambda^\dagger] = E^\lambda_{\rm QRPA} \hat{O}_\lambda^\dagger, \tag{8}$$

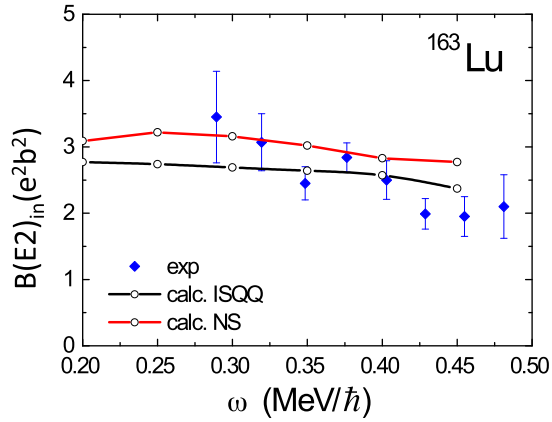

FIG. 3. (Color online) Experimental and calculated $B(E2)_{\rm in} = B(E2, I \to I-2)_{\rm in}$ values of the TSD band.

which yields the phonon excitation energies $E^\lambda_{\rm QRPA}$ and the phonon excitation operators $\hat{O}_\lambda^\dagger$ defined by

$$\hat{O}_\lambda^\dagger = \sum_{\mu=i<j} \left(X^\lambda_\mu \hat{b}^\dagger_\mu - Y^\lambda_\mu \hat{b}_\mu \right). \tag{9}$$

The amplitudes X^λ_μ and Y^λ_μ are found by solving the standard set of linear equations following from Eq. (8). The quasiparticle Hamiltonian $\hat{h}'$ and the full Hamiltonian $\hat{H}'$ commute with the signature operator $R_1 = \exp(-i\pi \hat{I}_1)$, which generates a 180-deg rotation about the cranking axis. Therefore, the quasiparticle states and the phonon excitations have good signature quantum numbers. The energetically lowest phonon state with negative signature $r = -1$ embodies the wobbling excitation which is characterized also by giving the largest cross-over transition strength $B(E2, I \to I-1) = B(E2)_{\rm out}$. Accordingly, only two-quasiparticle components with the combined signature $r = r_i r_j = -1$ contribute to the wobbling operator $\hat{O}^\dagger$ in Eq. (9). One has to make sure that the spurious rotational solution with the energy $E_{\rm QRPA} = \hbar\omega$ does not mix with the wobbling solution. Self-consistency of the mean field ensures this requirement.

The $E2/M1$ transition amplitudes from the TSD wobbling band to the TSD g band are obtained by evaluating the matrix elements,

$$\langle w | \hat{\mathcal{M}}_m(E2/M1) | 0 \rangle = \langle 0 | \hat{O}_w \hat{\mathcal{M}}_m(E2/M1) | 0 \rangle, \tag{10}$$

where $|w\rangle$ means the wobbling phonon state and $|0\rangle$ denotes the QRPA vacuum state at the cranking frequency ω. The transition operators are

$$\begin{aligned} \hat{\mathcal{M}}_m(E2) &= e_p r_p^2 Y_{2m}(p) + e_n r_n^2 Y_m(n), \\ \hat{\mathcal{M}}_m(M1) &= \frac{3}{4\pi} g_p^{(l)} \hat{l}_{1m}(p) + g_p^{(s)} \hat{s}_{1m}(p) + g_n^{(s)} \hat{s}_{1m}(n). \end{aligned} \tag{11}$$

The component m is assigned to the transition $I \to I - m$. Furthermore, the orbital g factor for $M1$ is $g_p^{(l)} = 1\mu_N$ for protons and 0 for neutrons. The spin g factors $g_p^{(s)}$ and $g_n^{(s)}$ are 0.7 times the values for the free proton or neutron. The reduced transition probabilities are

$$B(E2/M1, I \to I \mp 1) = |\langle w | \hat{\mathcal{M}}_{\pm 1}(E2/M1) | 0 \rangle|^2. \tag{12}$$

In the self-consistent version of QRPA, the ISQQ term in the Hamiltonian (1) generates both the deformed mean field and the residual interaction. As discussed above, its strength is fixed to the value $\kappa_\circ = 0.01960$ for the whole frequency range $\omega = 0.15$–0.5 MeV/$\hbar$. The factorized form of the ISQQ term reduces the solution of the QRPA equation to searching the zeros of the dispersion determinant, which are located at the QRPA energies $E_{\rm QRPA}$.

In Figs. 4–6 we present the QRPA results for the wobbling energies and the inter band $B_{\rm out}(E2, I \to I-1)$ and $B_{\rm out}(M1, I \to I-1)$ values. The reduced transition probabilities of the upward transitions $I \to I+1$ are at least one order smaller and not displayed. The calculated wobbling energies $E_{\rm QRPA}(\omega)$ follow the decreasing tendency of the measured ones, which is characteristic for transverse wobbling. However, they are substantially below the experiment. At $\omega = 0.45$ MeV the frequency becomes zero, which signalizes the change to a

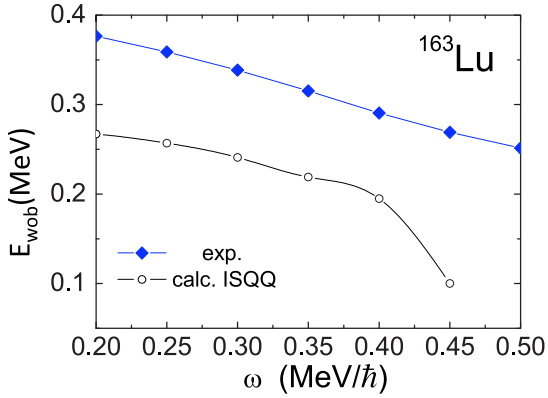

FIG. 4. (Color online) Excitation energy of the wobbling band in ^{163}Lu as a function of the rotational frequency. Experimental values (blue diamonds) are from [17]. QRPA calculation (solid line) with self-consistent ISQQ interaction.

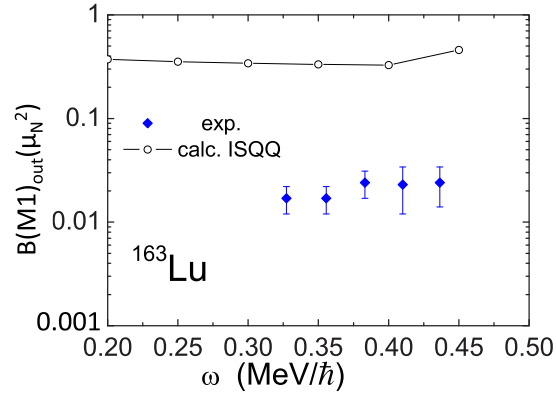

FIG. 6. (Color online) The reduced transition probabilities $B(M1)_{\rm out} = B(M1,(I \to I-1))_{\rm out}$ for the transitions between the TSD wobbling band to the TSD ground band in ^{163}Lu. Notations as in Fig. 4.

permanent tilt of the rotational axis away from the short axis. The experimental wobbling energies decrease linearly up to $\omega = 0.60$ MeV. The calculated ratios between the inter- and intraband transition probabilities $B(E2)_{\rm out}/B(E2)_{\rm in} = B(E2,I \to I-1)/B(E2,I \to I-2)$ reach only one-half of the measured values, whereas the calculated $B(M1,I \to I-1) = B(M1)_{\rm out}$ exceed the experimental ones by a factor 10. Our results are similar to the ones of Ref. [11], which used the QRPA version for ISQQ interaction in the body fixed frame. The deviations from experiment are about the same.

B. QRPA for Nilsson-Strutinsky deformations

The wobbling mode is sensitive to the ratios between the three moments of inertia, which strongly change with the triaxality parameter γ. The ISQQ coupling constant $\kappa_\circ = 0.01960$ used in the preceding section was adjusted to obtain a mean field deformation of $\varepsilon = 0.4$.

The self-consistent values of $\gamma \approx 10^\circ$ obtained with the coupling constant fixed this way are substantially smaller than the values $\gamma_{\rm pot}$ calculated by minimizing the Nilsson-Strutinsky energy functional, which are given in Table II. Following Refs. [13,14], we introduce the subscript "pot" to indicate that it is the triaxiality of the nuclear potential, which generally does not agree with the triaxiality of the density distribution $\gamma_{\rm den}$ (see below). References [13,14] demonstrated that larger values of $\gamma_{\rm pot}$ increase the ratio $B(E2)_{\rm out}/B(E2)_{\rm in}$ between the inter- and intraband transitions. Their QPPR version in the body fixed frame does not use the self-consistency in an explicit way, allowing them to freely choose the deformation of the mean field potential. To investigate this possibility in our framework we give up the self-consistency requirement, Eq. (4), between the shape parameters of the potential and the expectation values of quadrupole moments, which are implied by the QQ interaction in Eq. (2) with the common strength parameter κ_0. This means we use the same Nilsson Hamiltonian $\hat{h}$, Eq. (5), as before but the deformation parameters $(\varepsilon,\gamma_{\rm pot})$ shall be at our disposal. As pointed out by Refs. [13,14], one must distinguish between the triaxiality parameter $\gamma_{\rm pot}$ of the potential and the triaxiality parameter $\gamma_{\rm den}$ (see below) of the density distribution generated by the deformed potential, because the self-consistency requirement Eq. (4) was given up.

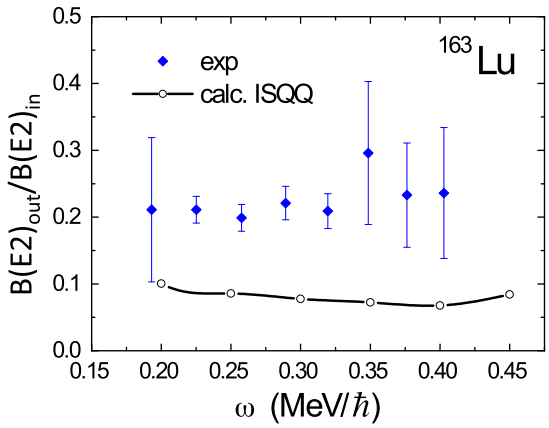

FIG. 5. (Color online) The ratios $B(E2)_{\rm out}/B(E2)_{\rm in}$ of the inter- and intraband reduced transition probabilities for the transitions between the TSD wobbling band and the TSD ground band in ^{163}Lu. Notations as in Fig. 4.

Self-consistency is only locally restored by constructing the residual interaction from the requirement that the resulting Hamiltonian $\hat{H} = \hat{h} + V_{4qp}$ becomes rotational invariant.

TABLE II. Deformation parameters $(\varepsilon,\gamma_{\rm pot})$ of ^{163}Lu in the frequency region $\omega = 0.15$–0.55 MeV/$\hbar$ obtained from a Nilsson-Strutinsky (NS) minimization [17].

ω(MeV/$\hbar$)	ε	$\gamma_{\rm pot}$(deg)
0.15	0.3815	18.75
0.2	0.3892	19.2
0.25	0.3968	19.64
0.3	0.4044	20.12
0.35	0.408	20.41
0.4	0.3991	20.72
0.45	0.3908	21.3
0.5	0.3852	21.78
0.55	0.3812	22.34

Such "symmetry-restoring interaction" [19,20],

$$V_{4qp} = -\frac{1}{2}\sum_{m=1}^{3}\kappa_m F_m^2, \tag{13}$$

is built from the squares of the commutators of the quasiparticle Hamiltonian $\hat{h}$ and the angular momentum components $J_{m=1,2,3}$:

$$F_m = [\hat{h}, i J_m]. \tag{14}$$

The strength constants κ_m are determined by demanding rotational invariance via the commutator,

$$[\hat{H}, i J_m] = \left[h - \frac{1}{2}\sum_{n=1}^{3}\kappa_n F_n^2, i J_m\right] = 0, \tag{15}$$

which can be satisfied on average $\langle[\hat{H}, i J_m]\rangle = 0$ by fixing the strength constants according to

$$\kappa_m^{-1} = \langle[[\hat{h}, i J_m], i J_m]\rangle, \tag{16}$$

where $|\rangle$ is the reference quasiparticle configuration.

This method can be applied to any mean field Hamiltonian $\hat{h}$, as, for instance, in Ref. [13] to a deformed Woods-Saxon potential. In our case the commutator (14) with a quadrupole deformed field generates again quadrupole operators. We evaluate the commutators relations (14, 16) explicitly. The results are written in terms of the combined quadrupole operators $Q_{1\pm}$ and $Q_{2\pm}$ defined by

$$\begin{aligned} Q_{1+} &= \frac{Q_1 + Q_{-1}}{i\sqrt{2}}, \quad Q_{1-} = \frac{Q_1 - Q_{-1}}{\sqrt{2}}, \\ Q_{2+} &= \frac{Q_2 + Q_{-2}}{\sqrt{2}}, \quad Q_{2-} = \frac{Q_2 - Q_{-2}}{i\sqrt{2}}. \end{aligned} \tag{17}$$

We introduce the constants $\mathcal{Q}$ and $\gamma_{\rm den}$, which specify the shape of the density distribution for given deformation parameters $(\varepsilon, \gamma_{\rm pot})$ of the potential,

$$\begin{aligned} \mathcal{Q} &= \sqrt{\langle Q_0\rangle^2 + \langle Q_{2+}\rangle^2}, \\ \sin\gamma_{\rm den} &= -\frac{\langle Q_{2+}\rangle}{\mathcal{Q}}, \quad \cos\gamma_{\rm den} = \frac{\langle Q_0\rangle}{\mathcal{Q}}. \end{aligned} \tag{18}$$

The Hamiltonian (1) with the interaction (13) takes the form,

$$\begin{aligned} \hat{H} = \hat{h} + \frac{1}{3}\frac{\hbar\omega_\circ\varepsilon}{\mathcal{Q}}\Bigg[&\frac{\sin\gamma_{\rm pot}}{\sin\gamma_{\rm den}}Q_{2-}^2 + \frac{\sin(\gamma_{\rm pot}+2\pi/3)}{\sin(\gamma_{\rm den}+2\pi/3)}Q_{1+}^2 \\ &+ \frac{\sin(\gamma_{\rm pot}-2\pi/3)}{\sin(\gamma_{\rm den}-2\pi/3)}Q_{1-}^2\Bigg], \quad , \end{aligned} \tag{19}$$

where the constants κ_m are expressed in terms of $\mathcal{Q}$ and $\gamma_{\rm den}$. Hence, the residual interaction of the Hamiltonian $\hat{H}$, needed for the QRPA, is fully determined by the single-particle Hamiltonian $\hat{h}$, in our case by the deformation parameters $(\varepsilon, \gamma_{\rm pot})$ of its potential.

The "symmetry-restoring interaction" includes the self-consistent treatment of the ISQQ Hamiltonian (2) as a special case. Using the notation (17), expression (2) becomes

$$\hat{H} = \hat{h} - \frac{\kappa_\circ}{2}\sum_{\mu=0,1\pm,2\pm}Q_\mu^2. \tag{20}$$

In comparison with Eq. (19) it contains the additional terms Q_0^2 and Q_{2+}^2 which drive the β-γ vibrations. In this case one has to search for deformations $(\varepsilon,\gamma)_{\rm sc}$ which comply with the self-consistent conditions [cf. Eq. (4)],

$$\frac{\kappa_\circ}{2} = \frac{1}{3}\frac{\hbar\omega_\circ\varepsilon}{\mathcal{Q}}, \qquad \sin\gamma_{\rm pot} = -\frac{\langle Q_{2+}\rangle}{\mathcal{Q}} = \sin\gamma_{\rm den}. \tag{21}$$

For the self-consistent deformation $(\varepsilon,\gamma)_{\rm sc}$ the common prefactor in the Hamiltonian (19) becomes equal to $\kappa_\circ/2$ and the three ratios of the Sin terms become one. Thus, for the self-consistent deformations the Hamiltonian $\hat{H}$, Eq. (2), is fully rotational invariant, and the commutator relations (15) are exactly satisfied.

At variance with the standard QQ Hamiltonian (2), the coupling strengths of the three interaction terms $Q_{k\pm}^2$ in Eq. (19) are not equal for arbitrary choice of the deformation parameters $(\varepsilon,\gamma_{\rm pot})$. With the values of $\kappa_{1,2,3}$ obtained from Eq.(16) rotational symmetry is achieved *locally* because the commutator relations (15) are satisfied on average. This is in accordance with the fact that the QRPA treats the wobbling motion as a small angle vibration. Local rotational invariance ensures that the spurious rotational excitations can be removed as the ones with the energies $E_{\rm QRPA} = 0$ and $\hbar\omega$ (as in the self-consistent case).

Below we present the results of a QRPA calculation with the Hamiltonian $\hat{H}$ of Eq. (19) using the deformation parameters $(\varepsilon,\gamma_{\rm pot})$ of Table II, which were found by a Nilsson-Strutinsky minimization [17]. The $\gamma_{\rm pot}$ values are about 10° larger than the corresponding ISQQ values.

The NS deformations give nearly constant intraband reduced transition probabilities of $B(E2)_{\rm in} = 3({\rm eb})^2$, which agree with the experimental values for $\omega = 0.3$ MeV, but do not reproduce the downward trend toward 2 $({\rm eb})^2$ at $\omega = 0.45$.

Figure 7 shows the calculated wobbling frequencies together with the experimental values. Compared to the wobbling frequencies of the sc ISQQ model (cf. Fig. 4) the calculation with the Nilsson-Strutinsky deformations gives a flatter ω dependence, and the breakdown of the QRPA is

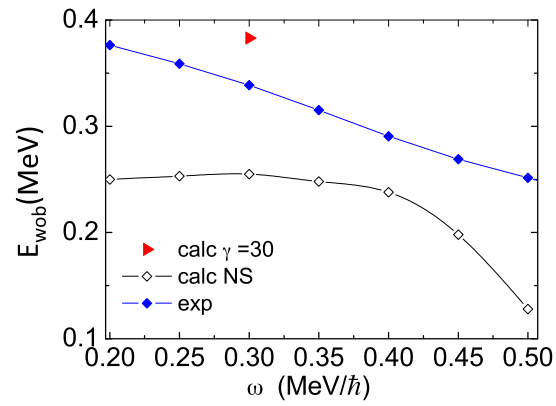

FIG. 7. (Color online) Wobbling frequencies in ^{163}Lu as a function of the rotational frequency. Experimental values (blue diamonds) are from [17]. The calculated values (solid line) are obtained with the Nilsson-Strutinsky (NS) deformations in Table II. The single value (red triangle) is found for the deformation point $(\epsilon = 0.4, \gamma = 30^\circ)$.

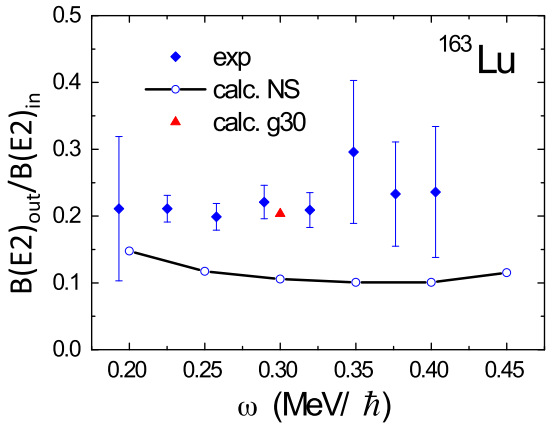

FIG. 8. (Color online) The ratios $B(E2)_{\rm out}/B(E2)_{\rm in}$ between the inter- and intraband reduced transition probabilities for the transitions between the TSD wobbling band and the TSD ground band in ^{163}Lu. Notations as in Fig. 7.

slightly retarded. As seen in Fig. 15 of our study [5], the QRPA wobbling frequency curve resembles the one obtained by applying the HFA approximation to the quasiparticle triaxial rotor (QTR) description of transverse wobbling in ^{163}Lu using microscopic moments of inertia calculated by means of the TAC model. The HFA is a small-amplitude approximation like QRPA. The full quantal solution of the QTR shows a gradual decrease of the wobbling frequency with frequency, which is closer to experiment (cf. Fig. 15 of [5]).

Comparing Fig. 5 with Fig. 8. shows that the larger $\gamma_{\rm pot}$ values lead to a 20% increase of the ratio $B(E2)_{\rm out}/B(E2)_{\rm in}$. No reduction is obtained for the magnetic interband transition strength as seen comparing Fig. 6 and Fig. 9. Hence with the larger $\gamma_{\rm pot}$ values predicted by the Nilsson-Strutinsky calculation and the symmetry restoring QRPA we only accomplish a marginally better description of the TSD band properties.

We tried the case of maximal triaxiality $\gamma_{\rm pot} = 30^\circ$ and $\varepsilon = 0.4$ for $\hbar\omega = 0.3$ MeV. The results are included in Figs. 7–9. The wobbling frequency is enlarged, somewhat exceeding the experimental value. The ratio $B(E2)_{\rm out}/B(E2)_{\rm in}$ is about right,

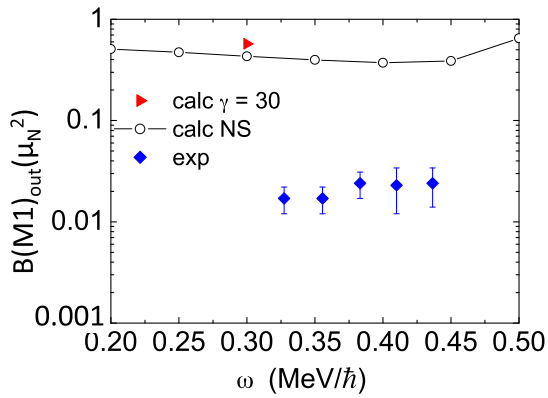

FIG. 9. (Color online) The reduced transition probabilities $B(M1)_{\rm out}$ for the transitions between the TSD wobbling band to the TSD ground band in ^{163}Lu. Notations as in Fig. 7.

such that it could be reproduced by choosing an appropriate $\gamma_{\rm pot}$ value between 25° and 30°. However, the small $B(M1)_{\rm out}$ values remain unexplained.

The result is consistent with the detailed analysis in Refs. [13,14] in the framework of QRPA based on the Nilsson and Woods-Saxon potentials and the pertinent symmetry restoring interaction. Using a triaxiality parameter of $\gamma_{\rm pot} \approx 20^\circ$ of the potential, which corresponds to the minimum of the deformation energy calculated by means of the shell correction method, gives $B(E2)_{\rm out}/B(E2)_{\rm in}$ ratios that underestimate the experimental ones by factors of 0.8 at $\omega = 0.2$ MeV and 0.5 at $\omega = 0.4$ MeV. The $B(M1)_{\rm out}$ values are a factor of 10 too large. Increasing by hand $\gamma_{\rm pot}$ from 20° at $\omega = 0.3$ MeV to 30° at $\omega = 0.5$ MeV reproduces the experimental values of both $B(E2)_{\rm out}$ and $B(E2)_{\rm in}$.

The authors trace back the small values of the ratio $B(E2)_{\rm out}/B(E2)_{\rm in}$ to a small value of $\gamma_{\rm den}$ calculated by means of Eqs. (18). It is important to note that the quadrupole moments derived from the microscopic density distribution appear in the transition probabilities. For the equilibrium deformations $\gamma_{\rm pot} = 20^\circ, 18^\circ$ (Nilsson, Woods-Saxon, respectively), they find $\gamma_{\rm den} = 12^\circ$. We obtain a similar small value of $\gamma_{\rm den} = 14^\circ$ from the expectation values of the quadrupole operator (11) with the quasiparticle reference state $|\varepsilon = 0.4, \gamma_{\rm pot} = 20^\circ\rangle$. The small increase of $\gamma_{\rm den}$ compared to the self-consistent ISQQ value of $\gamma = 10^\circ$ explains the only marginal increase of the $B(E2)_{\rm out}/B(E2)_{\rm in}$ ratios. The study of transverse wobbling in the framework of the QTR model demonstrated that a value of $\gamma_{\rm den} \approx 20^\circ$ is needed to reproduce the experimental $B(E2)_{\rm out}/B(E2)_{\rm in}$ ratios [5]. Such value is achieved by choosing $\gamma_{\rm pot} \approx 30^\circ$.

The self-consistency Eq. (4) ensures that $\gamma_{\rm pot} = \gamma_{\rm den}$ in the case of ISQQ. Therefore, the difference between $\gamma_{\rm pot}$ and $\gamma_{\rm den}$ reflects to a certain extent the missing self-consistency for arbitrarily adjusted values of $\gamma_{\rm pot}$. Self-consistency is incomplete for the shell correction method, which is used to calculate the equilibrium shapes of the Nilsson or Woods-Saxon potential. The difference $\gamma_{\rm pot}$ between $\gamma_{\rm den}$ may be smaller for a mean field basis that is derived from an effective interaction or density functional. This question has not been addressed so far. Calculations for ^{158}Er in the framework of the cranked relativistic mean field (CRMF) and cranked Skyrme-Hartree-Fock (CSHF) approaches gave small values of $|\gamma_{\rm den}| = 10^\circ$–$13^\circ$ for various configurations in ^{158}Er [21,22] and ^{160}Yb [23]. For the yrast configuration in ^{158}Er in the relevant spin range, CSHF gave $\gamma_{\rm den} = 12^\circ$ and the cranked Nilsson-Strutinsky approach $\gamma_{\rm pot} = 22^\circ$, which corresponds to $\gamma_{\rm den} \approx 12^\circ$ in good agreement with the CSHF value [21]. It seems that all cranked mean field approaches provide a shape with $\gamma_{\rm den} \approx 12^\circ$ in the TSD region.

The small triaxiality causes the too small $B(E2)_{\rm out}/B(E2)_{\rm in}$ ratios in the present QRPA calculations and the ones of Refs. [10–14]. The problem may be rooted either in the QRPA or in the mean field approaches, which would have farther-reaching consequences. To clarify the issue, QRPA calculations based on the CRMF or CSHF mean fields and a consistent residual interaction would be needed. Based on our QTR study in Ref. [5] we note the following. The small-amplitude approximation of QRPA is unlikely to be

responsible for the underestimation of the $B(E2)_{\rm out}/B(E2)_{\rm in}$ ratios, because the full large-amplitude solution gives a smaller ratio than the small-amplitude approximation (HFA) (see Fig. 17 there). The $B(E2)_{\rm out}/B(E2)_{\rm in}$ ratios depend on the wobbling amplitudes, which are determined by the ratios between the three moments of inertia. We carried out QTR calculation using the ratios between the moments of inertia calculated by means of the cranking model at the Nilsson-Strutinsky equilibrium deformation. The wobbling frequency is about 0.25 MeV (see Fig. 15 there) close to the value in Fig. 7 in the same frequency range, which may indicate that the wobbling amplitudes are similar. The QTR calculations, which used a ratio of $Q_2/Q_0 = \tan(\gamma_{\rm den} = 20^\circ)$, give $B(E2)_{\rm out}/B(E2)_{\rm in}$ ratios close to the experimental ones (see Fig. 17 there). In view of this, we consider the small ratio of $B(E2)_{\rm out}/B(E2)_{\rm in}$ obtained in our and the previous QRPA calculations as an open problem, possibly rooted in the mean field basis, and refrain from adjusting $\gamma_{\rm pot}$.

III. ADDITIONAL RESIDUAL INTERACTION TERMS

The experimental fact that the interband $M1$ transitions of the wobbling mode are strongly suppressed in comparison to the interband $E2$ transitions is a major motivation to study further interaction terms aside from the QQ interaction considered so far. The question is what makes the magnetic de-excitation so small. It is known that the scissors mode collects the low-lying $M1$ strength which is concentrated higher up in the energy region of 3–4 MeV [24,25]. A possible mechanism for suppressing the $M1$ strength of low-energy states is shifting it to the scissors mode, like the electric dipole strength of low-energy states is shifted to the giant dipole resonance.

Before presenting the results of our QRPA calculations with additional interaction terms a note about the removal of the spurious rotational modes is in order. When adding interaction terms the strength constants of which are not fixed by self-consistency or rotational invariance the rotational modes shift away from their true energies $E_{\rm QRPA} = 0, \hbar\omega$ and mix with the wobbling mode, such that the results are distorted by spurious effects. Therefore we apply the method proposed in Ref. [27] to eliminate the spurious modes. The QRPA Hamiltonian is complemented by the IS term $\kappa_j \mathbf{J}\cdot\mathbf{J}$ which acts like a spring force for the unwanted angle vibrations of the total angular momentum $\mathbf{J}$ in the rotating system. Choosing the stiffness parameter large, as $\kappa_j \geqslant 10^2$, the excitation energies for the rotational spurious states are shifted far outside the considered energy range, which prevents them from mixing with the physical modes.

Our first modification was motivated by the purely collective picture of the scissors mode being an angle vibration of the proton system against the neutron system with an IV QQ restoring force [26]. Accordingly, we added to the ISQQ Hamiltonian (2) an IV QQ interaction term built from the operators $\hat{Q}^{iv}_m = \hat{Q}_m(\pi) - \hat{Q}_m(\nu)$. Knowing the self-consistent strength $\kappa_\circ$ from Table I we set the isovector strength $\kappa^{iv}_\circ = r\,\kappa_\circ$ where the value of the ratio r was varied in the range -1.5 to -3.5 [1]. This addition lead to only a minor change of the $B(E2/M1)$ transition probabilities. However, it increased the wobbling frequency, such that the experimental wobbling frequencies could be fitted by choosing an appropriate value of r.

Second, we considered the spin-spin (SS) interaction, because it was successfully applied in connection with the scissors mode to explain the systematic accumulation of 1^+ states between 3 and 5 MeV with considerable $M1$ decay strength [20]. We included both the IS and the isovector (IV) SS interactions defined by

$$V^{(is,iv)}_{LL} = \sum_{m=-1,1} (-1)^m\, \hat{S}^{(is,iv)}_m \hat{S}^{(is,iv)}_{-m},$$
$$\hat{S}^{(is,iv)}_m = \hat{S}_m(\tau=+1) \pm \hat{S}_m(\tau=-1). \tag{22}$$

We determined the SS strength parameters by extrapolating the A-dependent strength parameters given in the work of De Coster and Heyde [29], used there for QRPA calculations of the 1^+. The SS interactions are then added to the self-consistent ISQQ Hamiltonian (2) described in Sec. II A. The results of the QRPA calculation for the frequency $\hbar\omega = 0.3\,{\rm MeV}/\hbar$ can be summarized as follows: The IS and IV SS terms have only negligible effects on both the wobbling energy and the $B(E2/M1)$ transition probabilities. The lowering of the $B(M1)_{\rm out}$ value is small, i.e., there is not much shift of the $M1$ strength into the scissor region.

Our third modification was motivated by the interpretation suggested in Ref. [26] that the scissors mode represents an angle vibration of the total *orbital* angular momentum vector $\mathbf{L}_\pi$ of the protons versus the *orbital* angular momentum vector $\mathbf{L}_\nu$ of the neutrons. Accordingly, we complemented the ISQQ Hamiltonian (2) by an interaction term that is composed of the isovector orbital angular momenta:

$$V_{LL} = \kappa_{LL}(\mathbf{L}_\pi - \mathbf{L}_\nu)^2. \tag{23}$$

Reference [30] successfully used an interaction of the type $V_{JJ} = \kappa_{JJ}(\mathbf{J}_\pi - \mathbf{J}_\nu)^2$ to describe the $M1$ strength in the scissors region of the Mo isotopes. We checked that such IV JJ interaction gives nearly the same results as the LL interaction when the coupling constant is appropriately chosen. This is not surprising, because it differs from the LL interaction by the spin operator. As discussed above, the inclusion of the IV SS interaction does not induce any substantial modification of the wobbling mode, which indicates that the spin degrees of freedom are not important for it.

The effects of adding the LL interaction are shown in Figs. 10–12. The calculated wobbling energy increases because of the repulsive LL term. We find a good match to the experimental curve when choosing the strength constant $\kappa_{LL} = 0.5\,{\rm MeV}/\hbar^2$. The interband $E2$ transitions stay almost unchanged, which is expected from a current-current interaction. The same value of κ_{LL} gives the desired suppression of the $B(M1)$ transition strength, which comes close to the measured values.

Hence, the QRPA with additional LL interaction is capable of providing a satisfactory description of the wobbling frequencies and of the magnetic properties. This raises the question whether the adjusted coupling parameter κ_{LL} is consistent with the experimental information about the scissors mode built on the ground states of the even-even neighbors.

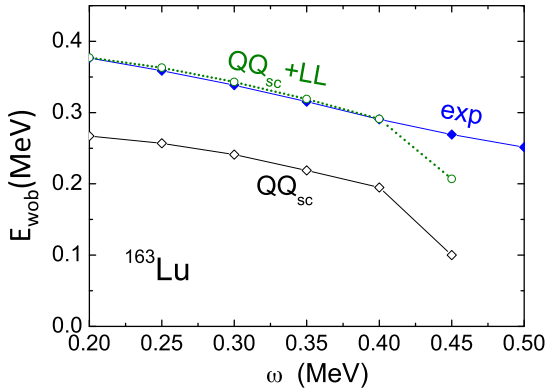

FIG. 10. (Color online) Wobbling frequencies in ^{163}Lu as a function of the rotational frequency. Experimental values (blue diamonds) are from [17]. Calculated values are obtained with QRPA using (solid line) self-consistent ISQQ interaction and (green dotted line) additionally LL interaction [see Eq. (23)].

We calculated the distribution of $B(M1, 0 \rightarrow 1^+)$ from the ground state of ^{162}Yb using the same QRPA approach as for the wobbling mode in ^{163}Lu. The deformation $\beta = 0.225$ from was taken from Ref. [28], and the value $\kappa_{LL} = 0.5\,\mathrm{MeV}/\hbar^2$ used for the LL interaction. The resulting distribution is shown in Fig. 13 for the interval $E = 2$–4 MeV, which is the suggested region of the scissors mode. There is no experimental information for the unstable nuclide ^{162}Yb about the distribution of 1^+ states to compare with. However, the systematics of the summed $B(M1)$ strength presented in Refs. [24,25] provides a clue concerning the coupling constant. Our value $\kappa_{LL} = 0.5\,\mathrm{MeV}/\hbar^2$ gives a summed strength $\Sigma B(M1) \approx 1.5\,\mu_N^2$ for the 1^+ excitations between 0 and 4 MeV, which agrees with the value from the systematics for the deformation $\beta = 0.225$ of ^{162}Yb. The agreement indicates that the coupling of the transverse wobbling to the scissors mode at high spin and the $M1$ strength of the low-spin scissors mode can be accounted for by one and the same value of κ_{LL}.

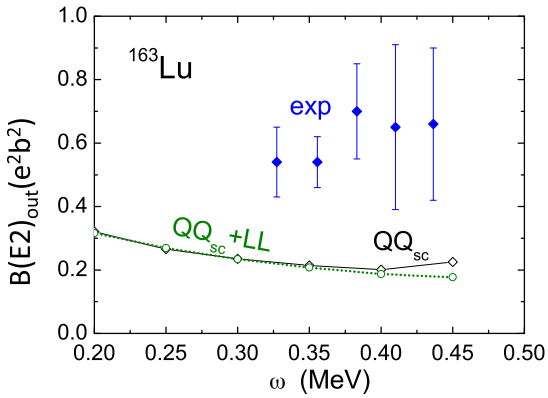

FIG. 11. (Color online) The reduced transition probabilities $B(E2)_{\mathrm{out}} = B(E2, I \rightarrow I-1)_{\mathrm{out}}$ for the transitions between the TSD wobbling band and the TSD ground band in ^{163}Lu. Calculated values are obtained with QRPA using (solid line) self-consistent ISQQ interaction and (green dotted line) additionally LL interaction [see Eq. (23)].

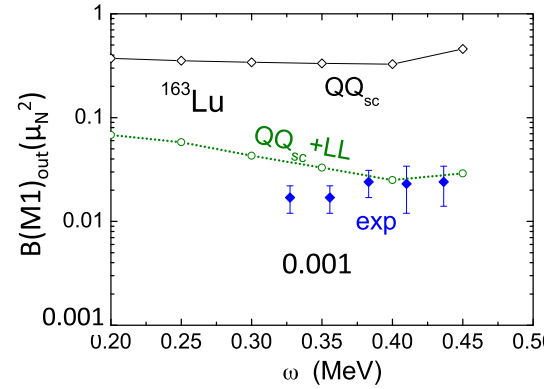

FIG. 12. (Color online) The reduced transition probabilities $B(M1)_{\mathrm{out}}$ for the transitions between the TSD wobbling band to the TSD ground band in ^{163}Lu. Calculated values are obtained with QRPA using (blue line) self-consistent ISQQ interaction and (green dotted line) additionally LL interaction [see Eq. (23)].

In the other case of a well-studied example of transverse wobbling, ^{135}Pr, the QTR calculations in Ref. [6], which do not take into account the coupling to the scissors mode, overestimate the $B(M1)_{\mathrm{out}}$ values by a factor of three. One expects a weaker coupling to the scissors mode, because ^{135}Pr is much less deformed than ^{163}Lu, and it is known that the $M1$ strength collected by the scissors mode increases quadratically with the deformation parameter [24,25].

The improvements achieved by including the IV LL interaction term can be taken as an indication that the wobbling motion is not a pure orientation vibration of the quadrupole mass tensor with respect to the angular momentum vector. It implies a coupling to vibrations of the proton and neutron currents against each other (see the interpretation of the scissors mode in Ref. [31]). The microscopical origin of such schematic interaction of the current-current type remains obscure at this point. As discussed above, taking into account oscillations of the neutron quadrupole tensor against the proton one also increases the wobbling frequency, but does

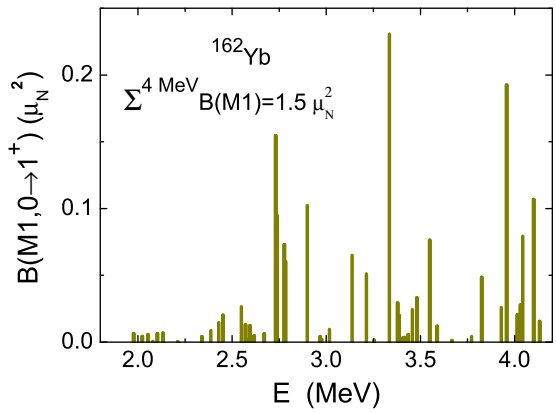

FIG. 13. (Color online) $B(M1)$ distribution of ^{162}Yb obtained by QRPA with the LL interaction, Eq. (23), choosing the strength constant $\kappa_{LL} = 0.5\,\mathrm{MeV}/\hbar^2$. The fragmented $B(M1)$ strength adds up from 0 to 4 MeV to a sum strength of $1.5\,\mu_N^2$ that can be interpreted as scissors strength.

not influence the magnetic properties. Regarding both, it would be interesting to see how QRPA-based modern density functionals and a consistent residual interaction describes transverse wobbling.

As discussed Sec. II B, increasing the triaxiality of the potential to $\gamma_{\rm pot} \approx 30^\circ$ by hand allows one to shift the $B(E2)_{\rm out}$ and $B(E2)_{\rm in}$ values to the experimental ones. Simultaneously, the wobbling frequency is shifted to somewhat above the experimental value. Taking into account the LL interaction in addition would result in a too high wobbling frequency. This is a good reason to refrain from adjusting $\gamma_{\rm pot}$.

Reference [32] reported a suppression of the $B(M1)_{\rm out}$ between rotational bands built on different members of the quasineutron $j_{15/2}$ multiplet in ^{235}U by a factor of 20–50 compared to estimates in the framework of the QTR model. In addition, the authors tabulated examples of $B(M1)_{\rm out}$ values between bands of high-j multiplet members, which all appear strongly suppressed. This systematic quenching of $M1$ strength suggests that the scissors mode draws $M1$ strength from the low-energy transitions in analogy to the quenching of the low-energy $E1$ transitions by coupling to the GDR (screening), which is the mechanism suggested for the wobbling mode here.

IV. SUMMARY AND CONCLUSIONS

The transverse wobbling mode in ^{163}Lu was reinvestigated in the framework of quasiparticle-random-phase approximation. The QRPA calculations were based on the rotating mean field that consisted of a deformed Nilsson potential and an attenuated monopole pair field. Various versions of the residual interaction were investigated. For all variants, the QRPA wobbling frequencies decreased with the rotational frequency, so confirming the transverse character of the solution.

First we studied an isoscalar quadrupole-quadrupole interaction and self-consistent deformation parameters. The results in essence agree with previous QRPA calculations [11], which used the same mean field Hamiltonian but another way of finding the solutions. The calculated wobbling frequencies show the right descent with the rotational frequency but are only 60% of the experimental excitation energy. The $B(E2)_{\rm out}/B(E2)_{\rm in}$ ratios for the interband transitions connecting the wobbling with the ground band and the intraband transitions show the characteristic collective enhancement, but are low by about a factor two. The $B(M1)_{\rm out}$ values of these interband transitions are a factor 10 too large compared with experiment.

Second, we determined the deformation parameters of the Nilsson potential by means of the Strutinsky method, which gives a triaxialty parameter of $\gamma_{\rm pot} \approx 20^\circ$. The factorized residual interaction was derived from the mean field by requiring local rotational invariance. The results slightly moved toward the experimental values, however, the discrepancies remained as substantial as before. We agree with the explanation of this insensitivity suggested in Refs. [13,14]. The increase of the triaxility of the potential from $\gamma_{\rm pot} = 10^\circ$ to 20° induces only a marginal increase of the triaxiality of the density distribution from $\gamma_{\rm den} = 10^\circ$ to 12°–13°, which is reflected by the small $B(E2)_{\rm out}/B(E2)_{\rm in}$ ratios. At this point we have to conclude that the reason for the low $B(E2)_{\rm out}/B(E2)_{\rm in}$ ratios remains unclear. Note that cranking calculations based on modern energy density functionals [21–23] find similar small triaxiality of the density in neighboring nuclides ^{158}Er and ^{160}Yb. QRPA calculations based on such self-consistent mean fields and an effective interaction derived from the density functional are needed to clarify the issue. In case they would also give too small $B(E2)_{\rm out}/B(E2)_{\rm in}$ ratios as found in this paper, this would reveal a serious problem of the mean field calculations for the TSD region. Configuration assignments based on the comparison with measured transition quadrupole moments for in-band transitions, as, for example, in Refs. [21,22], needed to be reconsidered, because they rely on the assumption that the calculations give the correct triaxiality of the density distribution.

Third, we included a repulsive isovector current-current interaction of the schematic form $\kappa_{LL}(\mathbf{L}_\pi - \mathbf{L}_\nu)^2$, where $\mathbf{L}$ is the total orbital angular momentum. This LL interaction couples the wobbling mode to the scissors mode, which represents a concentration of orbital $M1$ strength in the region E=3–4 MeV above the yrast line. The $B(M1)_{\rm out}$ values are reduced, because $M1$ strength is shifted into the scissors region, and the wobbling frequencies increase because the LL interaction is repulsive. The same interaction strength κ_{LL} generates the right upshift of the wobbling frequencies and the right suppression of the $B(M1)_{\rm out}$ values toward the experimental values. Moreover, using the same κ_{LL} value, QRPA on the ground state of the neighbor ^{162}Yb reproduces the cumulative $M1$ strength below 4 MeV, known from experimental systematics.

Altogether, QRPA based on the combination of the isoscalar QQ and isovector LL interactions well reproduces the experimental frequencies on transverse wobbling of the triaxial strongly deformed nuclide ^{163}Lu. It accounts for the strong suppression of the intraband $M1$ transitions. However, it underestimates the collectivity of the interband $E2$ transitions. The mode represents mainly an oscillation of the triaxial charge distribution relative to the angular momentum vector, which is manifest by strong $E2$ transitions from the one-phonon to the zero-phonon wobbling bands. Additionally, it contains a substantial admixture of scissorslike oscillations of the proton currents against the neutron currents, which increase the wobbling frequency and reduce the $M1$ transition strength between the wobbling bands by a factor of 10.

Note added. Before this manuscript was submitted, one of the co-authors, Fritz Dönau, passed away.

ACKNOWLEDGMENT

Support from US Department of Energy Grant No. DE-FG02-95ER40934 is acknowledged.

[1] A. Bohr and B. R. Mottelson, *Nuclear Structure*, Vol. II (Benjamin, New York, 1975).
[2] S. W. Ødegård *et al.*, Phys. Rev. Lett. **86**, 5866 (2001).
[3] H. J. Jensen *et al.*, Nucl. Phys. A **695**, 3 (2001).
[4] D. R. Jensen *et al.*, Nucl. Phys. A **703**, 3 (2002).
[5] S. Frauendorf and F. Dönau, Phys. Rev. C **89**, 014322 (2014).

[6] J. T. Matta *et al.*, Phys. Rev. Lett. **114**, 082501 (2015).
[7] I. Hamamoto, Phys. Rev. C **65**, 044305 (2002).
[8] I. Hamamoto and G. B. Hagemann, Phys. Rev. C **67**, 014319 (2003).
[9] K. Sugawara-Tanabe and K. Tanabe, Phys. Rev. C **82**, 051303 (2010).
[10] Y. R. Shimizu and M. Matsuzaki, Nucl. Phys. A **588**, 559 (1995).
[11] M. Matsuzaki, Y. R. Shimizu, and K. Matsuyanagi, Phys. Rev. C **65**, 041303(R) (2002).
[12] M. Matsuzaki and S.-I. Ohtsubo, Phys. Rev. C **69**, 064317 (2004)
[13] T. Shoji and Y. R. Shimizu, Prog. Theor. Phys. **121**, 319 (2009).
[14] Y. R. Shimizu, T. Shoji, and M. Matsuzaki, Phys. Rev. C **77**, 024319 (2008).
[15] D. Almehed, F. Dönau, and S. Frauendorf, Phys. Rev. C **83**, 054308 (2011).
[16] S. Frauendorf, Nucl. Phys. A **677**, 115 (2000).
[17] A. Görgen *et al.*, Phys. Rev. C **69**, 031301(R) (2004).
[18] P. Ring and P. Schuck, *The Nuclear Many-Body Problem* (Springer, New York, 1980).
[19] M. I. Baznat and N. I. Pjatov, Sov. J. Nucl. Phys. **21**, 365 (1975).
[20] R. Nojarov and A. Faessler, Nucl. Phys. A **484**, 1 (1988).
[21] Yue Shi *et al.*, Phys. Rev. Lett. **108**, 092501 (2012).
[22] A. V. Afanasjev, Y. Shi, and W. Nazarewicz, Phys. Rev. C **86**, 031304(R) (2012).
[23] Yue Shi *et al.*, Phys. Rev. C **88**, 034311 (2013).
[24] W. Ziegler, C. Rangacharyulu, A. Richter, and C. Spieler, Phys. Rev. Lett. **65**, 2515 (1990).
[25] K. Heyde, P. von Neumann-Cosel, and A. Richter, Rev. Mod. Phys. **82**, 2365 (2010).
[26] N. Lo Iudice and F. Palumbo, Phys. Rev. Lett. **41**, 1532 (1978).
[27] F. Dönau, Phys. Rev. Lett. **94**, 092503 (2005).
[28] P. Möller, J. R. Nix, W. D. Myers, and W. J. Swiatecki, At. Data Nucl. Data Tables **59**, 185 (1995).
[29] C. DeCoster and K. Heyde, Nucl. Phys. A **529**, 507 (1991).
[30] G. Rusev *et al.*, Phys. Rev. C **73**, 044308 (2006).
[31] I. Hamamoto and S. Aberg, Phys. Lett. B **145**, 163 (1984).
[32] D. Ward *et al.*, Phys. Rev. C **86**, 064319 (2012).